

Article

Comparing the Antibacterial Effect of Coated and Impregnated Flexible Dentures with Magnesium Oxide Nanoparticles against *Streptococcus mutans*

Zhala Dara Meran ¹, Pakhshan A. Hassan ²  and Ranj Nadhim Salaie ^{3,*} 

¹ Department of Prosthodontics, College of Dentistry, Hawler Medical University, Erbil 44001, Iraq; zhalla.meran@hmu.edu.krd

² Department of Biology, College of Science, Salahaddin University, Erbil 44001, Iraq; pakhsan.hassan@su.edu.krd

³ Department of Oral and Maxillofacial Surgery, Faculty of Dentistry, Tishk International University, Erbil 44001, Iraq

* Correspondence: ranj.nadhim@tiu.edu.iq; Tel.: +964-7504868610

Abstract: (1) Background: This study compares the antibacterial effect of coated and impregnated flexible dentures with magnesium oxide nanoparticles (MgONPs) against *Streptococcus mutans*. (2) Methods: the study used flexible denture material discs. The experimental groups were uncoated discs (control), 5% MgONPs coated discs (coated), and 5% MgONPs impregnated discs (impregnated). The homogenous distribution of MgONPs within the matrix was determined using scanning electron microscopy (SEM), and surface roughness and modulus elasticity were also measured. The antibacterial efficacy was tested against *Streptococcus mutans* in suspension and biofilm. The adhesion of microorganisms was assessed using an adherence assay test, optical light microscopy, and turbidity test. (3) Results: The nanoparticles were successfully coated or impregnated on the substrate and caused a significant increase in roughness. The effect of 5% MgONPs was significant ($p < 0.05$). The flexible denture samples whether coated or impregnated with 5% MgONPs effectively inhibited the growth of microorganisms. The *Streptococcus mutans* growth was 2.5 folds higher in control compared to coated samples, while *Streptococcus mutans* growth was 1.5 folds higher in control compared to impregnated samples. Furthermore, this study confirmed there was a homogenous distribution of MgONPs for both coated and impregnated groups. (4) Conclusions: It was found that addition of 5% MgONPs can prevent the attachment of *Streptococcus mutans* to flexible removable denture material. Additionally, the antibacterial effect was higher in the coated-samples compared to impregnated-samples.

Keywords: prosthodontics; dental materials; nano dentistry; nano coatings



Citation: Meran, Z.D.; Hassan, P.A.; Salaie, R.N. Comparing the Antibacterial Effect of Coated and Impregnated Flexible Dentures with Magnesium Oxide Nanoparticles against *Streptococcus mutans*. *Coatings* **2023**, *13*, 1429. <https://doi.org/10.3390/coatings13081429>

Academic Editor: Daniela Predoi

Received: 30 June 2023

Revised: 6 August 2023

Accepted: 8 August 2023

Published: 15 August 2023



Copyright: © 2023 by the authors. Licensee MDPI, Basel, Switzerland. This article is an open access article distributed under the terms and conditions of the Creative Commons Attribution (CC BY) license (<https://creativecommons.org/licenses/by/4.0/>).

1. Introduction

There are many options for replacing missing teeth, and removable dentures is one of them [1,2]. Various materials are available for denture fabrication. Polymethyl methacrylate (PMMA) has long been used as a denture material [3,4]. However, it has disadvantages such as insertion in undercut areas, brittleness, and allergy to methyl methacrylate monomer. In recent times, flexible removable partial dentures have become quite popular as they possess unique physical and esthetic properties as well as excellent retention. In spite of all these benefits, they have some difficulty in adjustment and polishing [5,6]. Thus, an unpolished surface will lead to the formation of irregularities and roughness. The surface roughness of prostheses will provide niches in which the microorganisms are protected from sheer forces and oral hygiene measures. Subsequently, the probability of bacterial accumulation will be increased compared to smooth surfaces [7,8]. Nowadays, nanotechnology can offer some advantages in improving biomaterials. Nanoparticles, due

to their small size and their colloidal behavior, exhibit an excellent adherence on the surfaces which facilitates their use in biomaterials as a coating or impregnation [9–11]. Furthermore, nanostructure biomaterials can produce better responses between the material surface and biological entities [12–15]. For example, MgO NPs exhibited biocidal activity against bacteria and spores [16,17]. The antibacterial activity of MgO NPs depends on many factors; among them, whether they are coated or impregnated into the biomaterial. There might be a difference in mechanical properties and/or antibacterial activity of nano-coated vs. impregnated biomaterials. Limited studies have been undertaken comparing the coated vs. impregnated nanoparticles on denture materials; also, limited MgONPs are used for this purpose. Thus, the main aim of this study was to investigate the antibacterial properties of coated and impregnated flexible dentures with MgO NPs against *Streptococcus mutans* without interfering with physical and mechanical properties.

2. Materials and Methods

2.1. Experimental Design

The experiment used flexible denture discs (Valplast International Corp, Nylon 12, East Northport, NY, USA) prepared according to the manufacturer's instructions. The experimental groups were; uncoated discs (control), 5% MgO NPs coated discs (coated), and 5% MgO NPs impregnated discs (impregnated), ($n = 10$). To test the antibacterial activity, *Streptococcus mutans* were grown on the surface of specimens for 24 h and then adherence of bacterial cells on the surface of specimens was investigated. To investigate the morphology and confluence of the bacterial cells after the experiment, another set of specimens was assigned to be examined under the microscope after 24 h growth on the control, coated, and impregnated specimens ($n = 3$).

2.2. Preparation of the Stock Dispersions and Nanoparticles Characterization

The magnesium oxide nanoparticles used for the experiments were purchased from Research Nano Material, Inc., US-3310-2020, Houston, TX, USA, with a purity of 99+% and 20 nm. Briefly, 1 g L⁻¹ stock dispersion of MgO NPs was initially prepared in ultrapure water. The stock solution was sonicated for 4 h to disperse the nanomaterials (35 kHz frequency, Fisherbrand FB 11010, Germany), before preparing secondary stocks of 5 mg L⁻¹, the MgO NPs were autoclaved (1218C for 15 min at 15 psi pressure) to ensure sterility.

2.3. Specimen Preparation

The samples were prepared in a disc shape with a diameter of 10 mm and thickness of 2 mm. For the first treatment group (coated), the specimens were prepared according to the manufacturer's instructions. To ensure sterility, each specimen was treated with 3 mL of 0.5% (*v/v*) chlorhexidine digluconate (R4, Septodont, Ltd., Maidstone, UK) for 5 min. Chlorhexidine digluconate was then aspirated from the surface of the specimen and the surface was washed twice with 5 mL of phosphate-buffered saline (PBS). Afterward, the disc surfaces were coated with MgO NPs aqueous solutions (5 mg L⁻¹) prepared in ultrapure water (see below). The coating process started by adding 2 mL of the MgO NPs solution on each disc for 24 h to allow particle precipitation on the specimen surface. Finally, the excess solution was gently aspirated to leave a thin MgO NP coating on the surface of the specimens. For the third treatment group (impregnated), 5% MgO NPs powder was added to the flexible denture; then, the samples were prepared according to the manufacturer's instructions. For the second and third groups after sample preparation, each disc was treated with 3 mL of 0.5% (*v/v*) chlorhexidine digluconate (R4, Septodont, Ltd., UK) for 5 min to ensure sterility. Chlorhexidine digluconate was then aspirated from the surface of the specimen and the surface was washed twice with 5 mL of phosphate-buffered saline (PBS).

2.4. Assessment of the Surface Roughness

The surface roughness of each specimen was measured by using a digital profilometer (Surftest-402; Mitutoyo, Kawasaki, Japan). The profiler was set to move a diamond stylus across the specimen surface under a constant load. Each line was scanned for 10 s with a constant force of 4 mN (0.4 gf) on the diamond stylus (stylus type = 5 μm radius). The value for the surface roughness was obtained from the digital scale. The Ra value (μm)—defined as “the mean value of all absolute distances of the roughness profiles from the mean line within the measuring distance”—is the figure for the overall roughness of a surface. Three measurements were taken for each specimen. The data were analyzed using one-way ANOVA (Version 16).

2.5. Assessment of the Modulus Elasticity

The modulus of elasticity of control, coated, and impregnated specimens ($n = 10$) was measured using the three-point bending test and by calculating the modulus of elasticity according to the formula $E = L3m/4bd^3$ with

E being modulus of elasticity (N/mm^2); L being support span (mm);

m being the gradient of the initial straight-line portion of the load detection curve (N/mm);

b being the width of the tested specimen (mm); d being the thickness of the tested specimen (mm).

A total of 10 specimens were tested.

2.6. Scanning Electron Microscopy (SEM)

A scanning electron microscope was used to determine the homogenous distribution of MgO NPs within flexible denture samples. For each group, five samples were prepared as described above. The samples had a dimension of 10 mm and 2 mm in thickness. The samples were cleaned in an ultra-sonicator in the organic solvent (alcohol) to remove any particular waste and residues. Then, they were mounted on SEM grids. The samples were coated with gold using an Emitech K550 gold sputter coater. Samples were imaged and elementally analyzed using an SEM, JEOL/JSM-7001F, Instruments INCA X-ray analysis system with a voltage of 20 KV, at a working distance of 10 mm. After the coating, the samples were mounted to the mounting stub using carbon paint. The sample was mounted to the device at 45° to produce a larger surface area for the electron beam to bombard the sample. Data analysis was performed using Aztec 2.0 software.

2.7. Isolation and Identification of *Streptococcus mutans* Clinical Strains

The bacteria were isolated from the dental plaque of a patient. The sample was taken from carious lesions using the tip of sterilized toothpicks. Subsequently, the toothpick was cut and then placed in 1 mL of sterile normal saline. The homogeneous suspension was obtained after vortexing the sample for one minute, and was then diluted by sterile phosphate-buffered saline and plated on blood agar and Mitis Salivarius agar (MSA) (Himedia, Mumbai, India), which was supplemented with 1% potassium tellurite solution. The plates were incubated anaerobically at 37°C for 48 h. After incubation, the colonies were morphologically checked and biochemically tested. Granular colonies with a frosted glass appearance exhibited either an alpha or gamma hemolysis pattern on blood agar, and hydrolyses aesculin was identified as *Streptococcus mutans*.

2.8. Preparation of Bacterial Suspensions

A single colony of *Streptococcus mutans* was inoculated in a brain–heart infusion broth (BHIB) in the screw-capped tube and incubated for 24 h. at 37°C . Then, a concentration of 1.5×10^8 CFU/mL was prepared. Once the bacteria were prepared, the samples were placed in each of the bacteriological cups. Each cup was filled with 15 mL BHI Brain Heart Infusion. Afterward, the samples (control, coated, and impregnated) were placed in the cups separately ($n = 10$). All cups were incubated for 24 h at 37°C under aerobic conditions.

After incubation, the samples were moved to new sterile cups filled with 15 mL fresh BHIB. Then, the biofilm was allowed to be grown for 24 h at 37 °C under aerobic conditions. At the end of the experiment, the samples were gently removed from the cups and rinsed by dipping them into the PBS solution 3 times for approximately 75 s in order to remove the unattached cells. To check whether a biofilm developed on the surface of the samples, the specimens were tested by adherence assay test and turbidity test.

2.9. Assessment of Mg Release

In the actual experiment, after 24 h bacterial exposure to the test groups, 0.4 mL of BHIB was collected and acidified with 20 µL of 70% nitric acid, and the Mg⁺² content of the aliquot was measured via inductively coupled plasma mass spectrometry ICP-MS (ICP-MS, X Series 2, Thermo Scientific, Hemel Hempstead, UK) against matrix-matched standards.

2.10. Adherence (Turbidity) Test

Adherence assay tests were used to investigate whether *Streptococcus mutans* had grown on the surface of the tested samples. The samples were removed from the plates and rinsed with PBS solution 3 times for approximately 75 s to remove the unattached cells. Then, for fixing the attached cells, specimens were treated with 100% ethanol for 3 s and left to dry in sterile plates. Specimens were stained using sterilized Methylene Blue stain (0.1%) for 1 min and, subsequently, were evaluated under the microscope (Olympus Microscope SZ-1145 CHI with transmitted light magnification 40×).

For turbidity assessment, spectrophotometry was used to obtain relative estimates of cell density. Since cells are turbid, less light will pass through the cuvette as the cell density increases. To estimate cell density after incubation, the specimens were gently removed from the cups and rinsed by dipping them into the PBS solution 3 times for approximately 75 s, then each sample was re-suspended in 2 mL of PBS and vortex shaken for 2 min at maximum speed to release cells from the samples. After that, the sample was removed and cells in the obtained solution were sonicated for 3 min to destroy cell aggregates, then the suspended biofilms were placed in 96-well plates and the absorbance was measured at 490 wavelengths. A turbidity test was conducted for both the suspended bacteria in BHIB and the attached (adhered) bacteria on the surface.

2.11. Statistical Analysis

Data are mean ± S.E.M and were analyzed using Statgraphics, version 16. Standard skewness and standard kurtosis were used to determine whether the data were normally distributed. One-way ANOVA and Tukey's test were used to locate significant differences between the variables using a 95% confidence limit. *p* values < 0.05 were considered statistically significant.

3. Results

The results showed that the nanoparticles were successfully applied on the substrate, which increased surface roughness of both coated and impregnated specimens but decreased the modulus elasticity while impregnated into the substrate. Moreover, there was a reasonable release of Mg to the external media. Regarding the antibacterial activity, both treatment groups showed significantly higher antibacterial activity compared to the control. Coated specimens were even more antibacterial than impregnated ones.

3.1. Specimen Characterization Using Scanning Electron Microscope (SEM)

The scanning electron microscope was used to determine the presence and homogeneous distribution of the MgO NPs within the flexible denture material for all the tested groups. The specimens were examined at zooming levels 600×, 20 KV. The SEM images of the control group showed a clear surface without any particles (Figure 1A). However, SEM images of coated samples showed the distribution of nanoparticles on the surface of

flexible denture samples (Figure 1B). Moreover, the impregnated samples also showed the presence of nanoparticles on the surface, as shown in (Figure 1C).

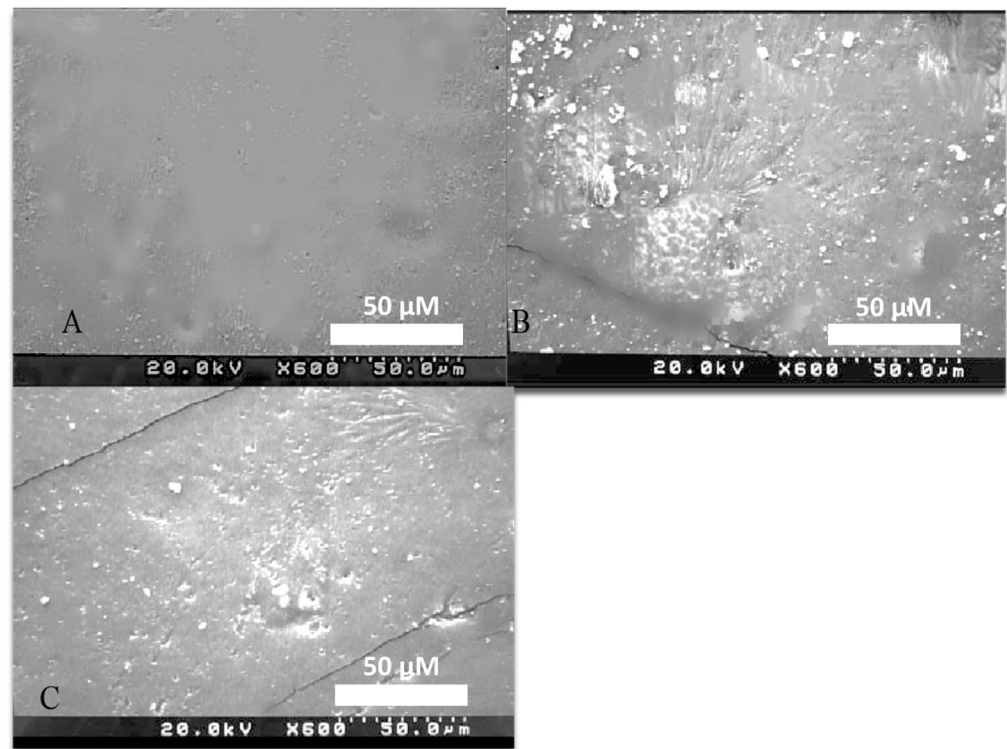


Figure 1. SEM Image of: (A) control flexible denture sample at 600× level. (B) Flexible denture sample coated with 5% MgO NPs at 600× level. (C) Flexible denture sample impregnated with 5% MgO NPs at 600× level.

3.2. Surface Roughness Values

According to the ANOVA results for the surface roughness values, there were significant differences among the groups ($p < 0.05$). The control group showed the lowest roughness value, while the impregnated and coated groups showed the highest roughness values. The surface roughness of the control was significantly lower than the modified samples (Table 1).

Table 1. Surface roughness (Ra) values of the specimens.

Groups	Surface Roughness, Ra (μm)
Control	0.31 ± 0.03 A
Coated	0.89 ± 0.04 B
Impregnated	0.72 ± 0.05 B

Data are mean \pm S.E.M. Different letters indicate significant differences between the groups ($n = 7$). One-way ANOVA ($p \leq 0.05$).

3.3. Modulus of Elasticity Values

The data revealed significant differences between coated and impregnated specimens ($p \leq 0.001$). However, there were no statistically significant differences between the control and coated samples (Figure 2).

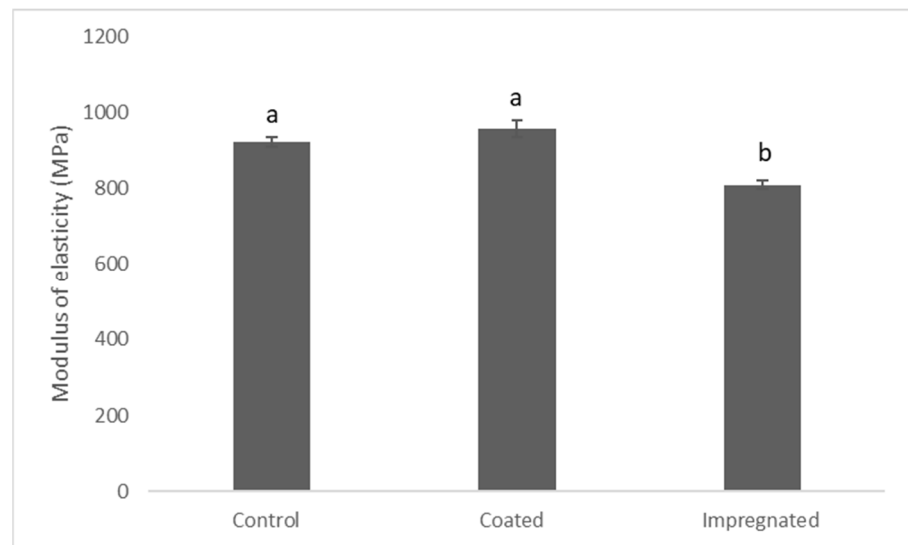


Figure 2. Modulus elasticity of the treatments. Data are mean \pm S.E.M. Different letters indicate significant differences between the groups (n = 7). One-way ANOVA ($p \leq 0.05$).

3.4. Assessment of Mg Release to the BHIB

Results showed that the Mg content of the external media was significantly higher in coated specimens compared to the impregnated specimens, measuring 0.6 ± 0.02 and 0.2 ± 0.03 , respectively. Mg content in the control was below the detection limit (Figure 3).

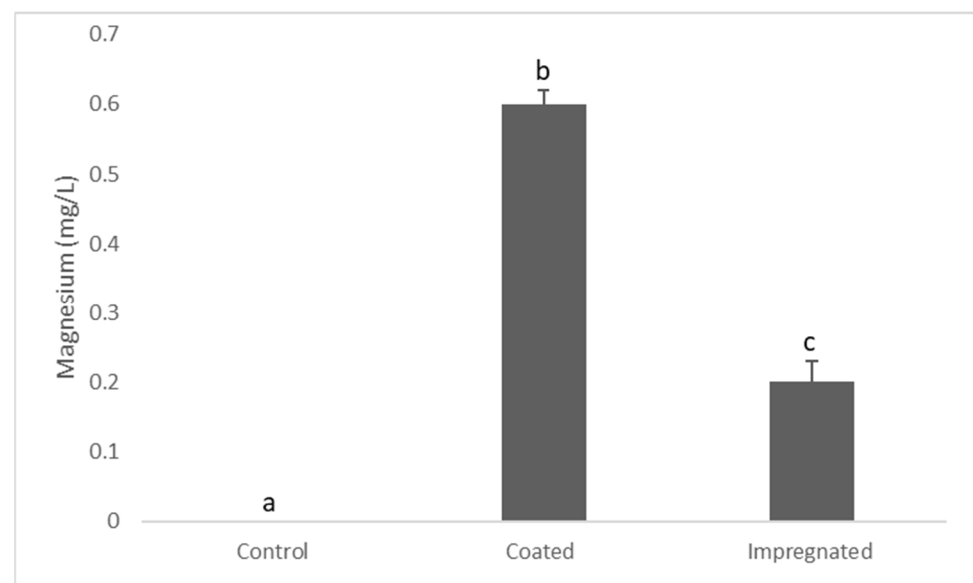


Figure 3. Magnesium concentration in the BHIB after 24 h. Data are mean \pm S.E.M. Different letters indicate significant differences between the groups. One-way ANOVA ($p \leq 0.05$).

3.5. Microscopic Examination of the Microbes on the Specimens

Microscopic growth of *Streptococcus mutans* was detected on all tested samples. Figure 4A shows that the cells (*Streptococcus mutans*) were well adhered to the surface of the control specimen. Cell confluence was increased in the control compared to coated and impregnated specimens. However, less growth was observed microscopically on coated and impregnated samples when compared with the control group. Nevertheless, less growth was seen on the coated samples when compared to impregnated samples, as shown in (Figure 4B,C).

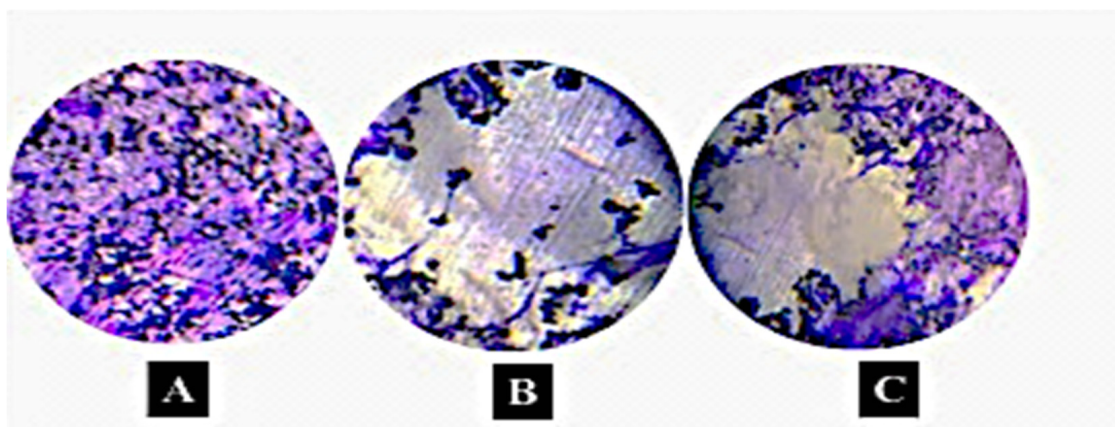


Figure 4. Microscopic images of *Streptococcus mutans* grown on flexible denture material. (A) *Streptococcus mutans* grown on control sample, (B) *Streptococcus mutans* grown on coated samples with 5% MgO NPs, (C) *Streptococcus mutans* grown impregnated sample with 5% MgO NPs. Note that the coated sample shows less bacterial coverage compared to others. The grey color means microbial-free surface (specimen surface). Olympus microscope SZ-1145 CHI with transmitted light magnification 40× was used (n = 3) scale bar = 10 μm.

3.6. Assessment of Antibacterial and Antibiofilm Activity

The turbidity values of the BHIB (suspension) in control, coated, and impregnated groups were 1.8 ± 0.2 , 0.2 ± 0.06 , and 1 ± 0.07 , respectively, and the coated group showed significantly less turbidity compared to the control (one-way ANOVA, $p = 0.001$), (Table 2). Regarding the turbidity in the biofilms, the turbidity of the control, coated, and impregnated samples was (0.55 ± 0.06), (0.1 ± 0.04), and (0.2 ± 0.02), respectively (Table 3). This indicates that there was more bacterial growth in the control compared to the coated and impregnated specimens. Moreover, bacterial growth on impregnated specimens was significantly more than on the coated specimens.

Table 2. Assessment of antibacterial properties of the coated/impregnated MgONP against *Streptococcus mutans* in suspension.

Groups	Absorbance at 595 nm
Control	1.8 ± 0.2 a
Impregnated	1 ± 0.07 b
Coated	0.2 ± 0.03 c

Data are mean \pm S.E.M (n = 10). Different letters indicate statistical difference from each other. One-way ANOVA $p \leq 0.05$.

Table 3. Assessment of antibiofilm activity of coated/impregnated MgO-NPs against *Streptococcus mutans*.

Groups	Absorbance at 595 nm
Control	0.55 ± 0.03 a
Impregnated	0.26 ± 0.01 b
Coated	0.14 ± 0.01 c

Data are mean \pm S.E.M (n = 10). Different letters indicate statistical difference from each other. One-way ANOVA $p \leq 0.05$.

4. Discussion

4.1. Coating Characterization and Mechanical Investigation

The presence and homogenous distribution of the MgO NPs were confirmed for both coated and impregnated samples with the use of a scanning electron microscope. The SEM images of coated samples showed even distribution of nanoparticles on the surface, and also formed small aggregations of nanoparticles, as shown in (Figure 1). Studies have demonstrated that the smallest metal oxide nanoparticles dissolve more readily, which creates a good distribution and explains the homogenous distribution of nanoparticles, as in this study, in which a small size nanoparticle (20 nm) was used for testing antimicrobial activity [18]. Furthermore, it was found that the metal oxide nanoparticles will aggregate, and it is a sensitive process [19]. The quantity of nanoparticles added to materials affects their aggregation, as the aggregation reaches the minimum in the case of moderate polymer–filler interaction, which will result in a good dispersion. However, adding more will increase the aggregation of the nanoparticles. Furthermore, this study showed that the coated samples showed more aggregation of nanoparticles than the impregnated samples (Figure 1B,C), and this result was expected, as [20] stated that small size and large surface area can lead to particle-particle aggregation, making physical handling of nanoparticles difficult in liquid and dry forms. Nevertheless, in the impregnated samples, it was shown that traditionally, the dispersion of particles in polymeric materials is difficult and frequently results in agglomeration, and this aggregation may be due to the attraction forces between the nanoparticles themselves and between molecules of the polymers [21]. In addition, it may be due to the high adsorption surface energies associated with these nanofillers, resulting in a strong tendency to form agglomerates and aggregates. Regarding the modulus elasticity, coated samples showed significantly higher elasticity compared to the impregnated ones. This finding is supported by another study which found that Mg nanoparticles agglomerate after impregnation in silicone specimens and, hence, negatively affect the elasticity [22].

4.2. Antimicrobial Activity

This study showed that the growth of *Streptococcus mutans* on the samples was confirmed microscopically, and it was well-adhered to the surface of samples, indicating easy adherence of microbes to the flexible denture samples surface after incubation. Like any other medical device, when flexible denture material is introduced into the body, it will be susceptible to biofilm formation since it is in contact with the mucosa in the oral cavity. The explanation of microbes' adherence to the surface of samples is due to many factors, such as the high surface hydrophobicity of samples, which interacts strongly with macromolecules and adsorbs considerable quantities of protein from the surrounding biological environment [23]. The protein-coated biomaterial can accelerate the initial attachment of microorganisms resulting in a formation of a biofilm layer on the surface [24–26]. Regarding the Mg release to the BHIB, it was found that around 0.5 ppm of Mg was released from the coated and impregnated specimens. A similar finding was observed in another study, which measured 0.3 ppm of silver release from silver-coated titanium dental implant disks to the BHIB. This cause of metal ion release to the biological media in the presence of organic molecules that accelerates the metal ion release [27].

In this study, both coated and impregnated specimens showed less bacterial adhesion compared to the control samples, indicating that when samples were modified with MgO NPs, they acted as an antimicrobial against *Streptococcus mutans*. This finding is supported by another study, which found that MgO nanoparticles incorporated into glass ionomer cement exhibited significantly more antibacterial activity against *Streptococcus mutans* [28]. This could be explained by a number of mechanisms, such as the release of reactive oxygen species (ROS), which is proposed to be the dominant mechanism. Furthermore, ion release from the nanoparticles can cause bacterial death through binding to the cell membrane [29,30]. Additionally, it has been stated that the increase of the surface area of MgO particles leads to more effective destruction of the cell wall of the bacteria [31],

as a larger surface area releases more ions. It was found that the electrostatic interaction between the bacterial surface and MgO nanoparticles causes cell death [32].

Moreover, MgO-NPs could take up halogen gases due to the defective nature of their surface and their positive charge, resulting in a strong interaction with bacteria. Furthermore, ref. [33] also stated that the MgO-NPs were adsorbed and dispersed on the bacterial cell walls, leading to the destruction or disintegration of the cell walls, and then they penetrated the bacterial cells, leading to leakage of the intracellular contents, which eventually resulted in cell death. Furthermore, it was demonstrated that the antimicrobial activity of MgO-NPs can be due to the alkaline effect and the discharge of Mg^{2+} upon the entrance of microbial cells [34].

Another explanation for the antimicrobial effect of the MgO NPs is their small size. It was stated that MgO-NPs, due to their extremely small size, allow many particles to cover the bacteria cells to a high extent and bring halogen in an active form in high concentration in proximity to the cell [16]. Studies also showed that the size of nanoparticles is very effective and plays an important role in antimicrobial effect, and the smaller the size, the more antimicrobial effect it shows [35]. The antibacterial property of MgO-NPs increases as the particle size decreases. Thus, the antimicrobial effect of MgO-NPs in this study could be explained by the fact that small-size nanoparticles (20 nm) were able to penetrate and damage bacteria cells. A similar study demonstrated that small MgO nanoparticles had an efficient antibacterial activity against *Escherichia coli* (*E. coli*) and *Staphylococcus aureus* (*S. aureus*), and they confirmed that when the small size of MgO nano-particles was used, better antibacterial activity would be observed toward *E. coli* and *S. aureus*. In addition, nanoparticles were observed in the cytoplasm of bacteria and suggested that these nanoparticles penetrated the cell wall and re-formed from individual MgO nano-particles, indicating a clear size effect on antibacterial activity [36].

It was clarified that the antimicrobial effect could be due to the high surface area of nanoparticles. Once the size of MgO NPs decreases, the surface area increases [37]. Thus, the increase in surface area determines the potential number of reactive groups on the particle surface, which are expected to show high antibacterial activity. It was also found that when the particle size of MgO is under 15 nm, the surface energy increases, leading to an increase in the aggregation effect [38]. Once a larger particle size is formed due to aggregation, the interaction with bacteria will be inhibited and the bactericidal efficiency becomes lower [39]. In addition to the particle size-dependent antibacterial effect of MgO nanoparticles, the dosage-dependent antibacterial activity of MgO-NPs was also confirmed. For instance, a study demonstrated the antibacterial effect of MgO nanoparticles against *E. coli* with a dosage of 7.5 $\mu\text{g}/\text{mL}$ –17.5 $\mu\text{g}/\text{mL}$ and confirmed that these doses can be used in medical applications [40]. Additionally, it was verified that 3 mg/mL MgO nanoparticles would be enough to kill all bacterial cells of *Escherichia coli* and *Salmonella* [41]. Thus, in this study, 5% MgO NPs were used and showed an antibacterial effect against *Streptococcus mutans*, and this dosage for both groups (coated and impregnated) was enough to cause loss of bacterial attachment to the surface of the samples.

This study also confirmed that when the samples were coated, more bacterial de-attachment was observed compared to impregnated samples with the same dosage of MgO nanoparticles. A study showed that the rationale behind adding nanoparticles to the samples is to inhibit or retard the growth of microorganisms, and the SEM images showed that most agglomeration occurred on the surface compared to on the core surface [42]. The significantly higher antibacterial activity of the coated compared to the impregnated specimens could be explained by the fact that coated samples release more ions than impregnated ones and also because of the higher direct contact between the nanoparticles and the microbes.

5. Conclusions

The coating/impregnation process was successful and caused a significant increase in the surface roughness. Within the limitations of this study, it was concluded that the

addition of 5% MgO NPs can prevent the attachment of *Streptococcus mutans* to a flexible denture prosthesis. In clinical situations, bacterial and fungal infections occur at lower doses, suggesting that the current dosage would be very effective indeed, and perhaps a lower concentration of MgO NPs could be used also. Furthermore, this study confirmed that the antibacterial effect of the MgO NPs as a coating was higher than impregnated flexible denture materials.

Author Contributions: Conceptualization, Z.D.M. and R.N.S.; formal analysis, Z.D.M., P.A.H. and R.N.S.; investigation, Z.D.M., P.A.H. and R.N.S.; data curation, Z.D.M., P.A.H. and R.N.S.; writing—original draft preparation, Z.D.M.; writing—review and editing, R.N.S.; supervision, R.N.S. All authors have read and agreed to the published version of the manuscript.

Funding: This research received no external funding.

Institutional Review Board Statement: Not applicable.

Informed Consent Statement: Not applicable.

Data Availability Statement: Not applicable.

Conflicts of Interest: The authors declare no conflict of interest.

References

1. Al-Quran, F.A.; Al-Ghalayini, R.F.; Al-Zu'bi, B.N. Single-tooth replacement: Factors affecting different prosthetic treatment modalities. *BMC Oral Health* **2011**, *11*, 34. [[CrossRef](#)]
2. Pereira, A.L.C.; de Medeiros, A.K.B.; de Sousa Santos, K.; de Almeida, É.O.; Barbosa, G.A.S.; Carreiro, A.D.F.P. Accuracy of CAD-CAM systems for removable partial denture framework fabrication: A systematic review. *J. Prosthet. Dent.* **2021**, *125*, 241–248. [[CrossRef](#)]
3. Sabri, B.; Satgunam, M.; Abreeza, N.M.; NAbed, A. A review on enhancements of PMMA denture base material with different nano-fillers. *Cogent Eng.* **2021**, *8*, 1875968. [[CrossRef](#)]
4. Singh, J.P.; Dhiman, R.K.; Bedi, R.P.S.; Girish, S.H. Flexible denture base material: A viable alternative to conventional acrylic denture base material. *Contemp. Clin. Dent.* **2011**, *2*, 313. [[CrossRef](#)] [[PubMed](#)]
5. Sharma, A.; Shashidhara, H.S. A review: Flexible removable partial dentures. *J. Dent. Med. Sci.* **2014**, *13*, 58–62.
6. Lim, G.S.; Buzayan, M.M.A.; Elkezza, A.; Sekar, K. The development of flexible denture materials and concept: A narrative review. *J. Health Transl. Med.* **2021**, *24*, 23–29. [[CrossRef](#)]
7. Abhay, P.N.; Karishma, S. Comparative evaluation of impact and flexural strength of four commercially available flexible denture base materials: An in vitro study. *J. Indian Prosthodont. Soc.* **2013**, *13*, 499–508. [[CrossRef](#)]
8. Vojdani, M.; Giti, R. Polyamide as a denture base material: A literature review. *J. Dent.* **2015**, *16* (Suppl. S1), 1–9.
9. Handy, R.D.; Shaw, B.J. Toxic effects of nanoparticles and nanomaterials: Implications for public health, risk assessment and the public perception of nanotechnology. *Health Risk Soc.* **2007**, *9*, 125–144. [[CrossRef](#)]
10. Meran, Z.; Besinis, A.; De Peralta, T.; Handy, R.D. Antifungal properties and biocompatibility of silver nanoparticle coatings on silicone maxillofacial prostheses in vitro. *J. Biomed. Mater. Res. Part B Appl. Biomater.* **2018**, *106*, 1038–1051. [[CrossRef](#)]
11. Zhao, C.; Xi, M.; Huo, J.; He, C.; Fu, L. Electro-reduction of N₂ on nanostructured materials and the design strategies of advanced catalysts based on descriptors. *Mater. Today Phys.* **2022**, *22*, 100609. [[CrossRef](#)]
12. Salaie, R.N.; Besinis, A.; Le, H.; Tredwin, C.; Handy, R.D. The biocompatibility of silver and nanohydroxyapatite coatings on titanium dental implants with human primary osteoblast cells. *Mater. Sci. Eng. C* **2020**, *107*, 110210. [[CrossRef](#)] [[PubMed](#)]
13. Engel, E.; Michiardi, A.; Navarro, M.; Lacroix, D.; Planell, J.A. Nanotechnology in regenerative medicine: The materials side. *Trends Biotechnol.* **2008**, *26*, 39–47. [[CrossRef](#)] [[PubMed](#)]
14. Fadeel, B.; Garcia-Bennett, A.E. Better safe than sorry: Understanding the toxicological properties of inorganic nanoparticles manufactured for biomedical applications. *Adv. Drug Deliv. Rev.* **2010**, *62*, 362–374. [[CrossRef](#)]
15. Calabrese, C.; La Parola, V.; Testa, M.L.; Liotta, L.F. Antifouling and antimicrobial activity of Ag, Cu and Fe nanoparticles supported on silica and titania. *Inorganica Chim. Acta* **2022**, *529*, 120636. [[CrossRef](#)]
16. Ravishankar Rai, V.; Jamuna Bai, A. *Nanoparticles and Their Potential Application as Antimicrobials*; A Méndez-Vilas, A., Ed.; Formatex: Mysore, India, 2011.
17. Naguib, G.H.; Nassar, H.M.; Hamed, M.T. Antimicrobial properties of dental cements modified with zein-coated magnesium oxide nanoparticles. *Bioact. Mater.* **2022**, *8*, 49–56. [[CrossRef](#)]
18. Kumar, R.; Pulikanti, G.R.; Shankar, K.R.; Rambabu, D.; Mangili, V.; Kumbam, L.R.; Sagara, P.S.; Nakka, N.; Yogesh, M. Surface coating and functionalization of metal and metal oxide nanoparticles for biomedical applications. In *Metal Oxides for Biomedical and Biosensor Applications*; Elsevier: Amsterdam, The Netherlands, 2022; pp. 205–231.
19. Jaragh-Alhadad, L.A.; Falahati, M. Tin oxide nanoparticles trigger the formation of amyloid β oligomers/protofibrils and underlying neurotoxicity as a marker of Alzheimer's diseases. *Int. J. Biol. Macromol.* **2022**, *204*, 154–160. [[CrossRef](#)]

20. Mohanraj, V.J.; Chen, Y. Nanoparticles—A review. *Trop. J. Pharm. Res.* **2006**, *5*, 561–573. [[CrossRef](#)]
21. Mackay, A.; Tuteja, P.M.; Duxbury, C.J.; Hawker, B.; Van Horn, Z.; Guan, G.; Chen, R. Krishnan, General strategies for nanoparticle dispersion. *Science* **2006**, *311*, 1740–1743. [[CrossRef](#)]
22. Meran, Z.; Salem, S.A. The Effect of Magnesium Oxide Nanoparticles Impregnated into Silicone Facial Prostheses against *Candida Albicans* and *Staphylococcus Epidermidis*. *Crescent J. Med. Biol. Sci.* **2020**, *6*, 466–472.
23. Gruebele, M. Protein folding and surface interaction phase diagrams in vitro and in cells. *FEBS Lett.* **2021**, *595*, 1267–1274. [[CrossRef](#)] [[PubMed](#)]
24. Soustre, J.; Rodier, M.-H.; Imbert-Bouyer, S.; Daniault, G.; Imbert, C. Caspofungin modulates in vitro adherence of *Candida albicans* to plastic coated with extracellular matrix proteins. *J. Antimicrob. Chemother.* **2004**, *53*, 522–525. [[CrossRef](#)] [[PubMed](#)]
25. Dominic, R.; Shenoy, S.; Baliga, S. *Candida* biofilms in medical devices: Evolving trends. *Kathmandu Univ. Med. J.* **2007**, *5*, 431–436.
26. Su, G.; Deng, X.; Zhong, H.; Hu, L.; Li, S.; Praburaman, L.; He, Z.; Sun, W. Ag⁺ significantly promoted the biofilm formation of thermoacidophilic archaeon *Acidianus manzaensis* YN-25 on chalcopyrite surface. *Chemosphere* **2021**, *276*, 130208. [[CrossRef](#)]
27. Salaie, R.N.; Hassan, P.A.; Meran, Z.D.; Hamad, S.A. Antibacterial Activity of Dissolved Silver Fractions Released from Silver-Coated Titanium Dental Implant Abutments: A Study on *Streptococcus mutans* Biofilm Formation. *Antibiotics* **2023**, *12*, 1097. [[CrossRef](#)]
28. Noori, A.J.; Kareem, F.A. The effect of magnesium oxide nanoparticles on the antibacterial and antibiofilm properties of glass-ionomer cement. *Heliyon* **2019**, *5*, e02568. [[CrossRef](#)]
29. Emamifar, A.; Kadivar, M.; Shahedi, M.; Solaimanianzad, S. Effect of nanocomposite packaging containing Ag and ZnO on inactivation of *Lactobacillus plantarum* in orange juice. *Food Control* **2011**, *22*, 408–413. [[CrossRef](#)]
30. Godoy-Gallardo, M.; Eckhard, U.; Delgado, L.M.; de Roo Puente, Y.J.; Hoyos-Nogués, M.; Gil, F.J.; Perez, R.A. Antibacterial approaches in tissue engineering using metal ions and nanoparticles: From mechanisms to applications. *Bioact. Mater.* **2021**, *6*, 4470–4490. [[CrossRef](#)]
31. Zhang, H.; Hu, J.; Xie, J.; Wang, S.; Cao, Y. A solid-state chemical method for synthesizing MgO nanoparticles with superior adsorption properties. *RSC Adv.* **2017**, *9*, 2011–2017. [[CrossRef](#)]
32. Priyadarshini, B.; Patra, T.; Sahoo, T.R. An efficient and comparative adsorption of Congo red and Trypan blue dyes on MgO nanoparticles: Kinetics, thermodynamics and isotherm studies. *J. Magnes. Alloys* **2021**, *9*, 478–488. [[CrossRef](#)]
33. Cai, L.; Chen, J.; Liu, Z.; Wang, H.; Yang, H.; Ding, W. Magnesium oxide nanoparticles: Effective agricultural antibacterial agent against *Ralstonia solanacearum*. *Front. Microbiol.* **2018**, *9*, 790. [[CrossRef](#)] [[PubMed](#)]
34. Hassan, S.E.D.; Fouda, A.; Saied, E.; Farag, M.; Eid, A.M.; Barghoth, M.G.; Awad, M.A.; Hamza, M.F.; Awad, M.F. Rhizopus Oryzae-mediated green synthesis of magnesium oxide nanoparticles (MgO-NPs): A promising tool for antimicrobial, mosquitocidal action, and tanning effluent treatment. *J. Fungi* **2021**, *7*, 372. [[CrossRef](#)] [[PubMed](#)]
35. Hosseini, S.N.; Pirsia, S.; Farzi, J. Biodegradable nano composite film based on modified starch-albumin/MgO; antibacterial, antioxidant and structural properties. *Polym. Test.* **2021**, *97*, 107182. [[CrossRef](#)]
36. Makhluif, S.; Dror, R.; Nitzan, Y.; Abramovich, Y.; Jelinek, R.; Gedanken, A. Microwave-assisted synthesis of nanocrystalline MgO and its use as a bactericide. *Adv. Funct. Mater.* **2005**, *15*, 1708–1715. [[CrossRef](#)]
37. Sharmin, S.; Rahaman, M.M.; Sarkar, C.; Atolani, O.; Islam, M.T.; Adeyemi, O.S. Nanoparticles as antimicrobial and antiviral agents: A literature-based perspective study. *Heliyon* **2021**, *7*, e06456. [[CrossRef](#)]
38. Yamamoto, O.; Fukuda, T.; Kimata, M.; Sawai, J.; Sasamoto, T. Antibacterial characteristics of MgO-mounted spherical carbons prepared by carbonization of ion-exchanged resin. *J. Ceram. Soc. Jpn.* **2001**, *109*, 363–365. [[CrossRef](#)]
39. Zakharova, O.; Kolesnikov, E.; Vishnyakova, E.; Strekalova, N.; Gusev, A. Antibacterial activity of ZnO nanoparticles: Dependence on particle size, dispersion media and storage time. *IOP Conf. Ser. Earth Environ. Sci.* **2019**, *226*, 012062. [[CrossRef](#)]
40. Maji, J.; Pandey, S.; Basu, S. Synthesis and evaluation of antibacterial properties of magnesium oxide nanoparticles. *Bull. Mater. Sci.* **2020**, *43*, 25. [[CrossRef](#)]
41. Jin, T.; He, Y.P. Antibacterial activities of magnesium oxide (MgO) nanoparticles against foodborne pathogens. *J. Nanopart. Res.* **2011**, *13*, 6877–6885. [[CrossRef](#)]
42. Rozilah, A.; Jaafar, C.N.; Sapuan, S.M.; Zainol, I.; Ilyas, R.A. The effects of silver nanoparticles compositions on the mechanical, physiochemical, antibacterial, and morphology properties of sugar palm starch biocomposites for antibacterial coating. *Polymers* **2020**, *12*, 2605. [[CrossRef](#)]

Disclaimer/Publisher’s Note: The statements, opinions and data contained in all publications are solely those of the individual author(s) and contributor(s) and not of MDPI and/or the editor(s). MDPI and/or the editor(s) disclaim responsibility for any injury to people or property resulting from any ideas, methods, instructions or products referred to in the content.